

1
2
3
4
5
6
7
8
9
10
11
12
13
14
15
16
17
18
19
20
21
22
23
24
25
26
27
28
29
30
31
32
33
34
35
36
37
38
39
40
41
42
43
44
45

Mallory A. Sea
King Abdullah University of Science and Technology
Red Sea Research Center (RSRC)
Thuwal, Saudi Arabia, 23955-6900
712-203-6729
mas012@morningside.edu

Prof. Michael Bahn
Co-editor-in-chief, *Biogeosciences*

Dear Prof. Michael Bahn,

Please find attached a revised version of the manuscript, “**Carbon Dioxide and Methane Emissions from Red Sea Mangrove Sediments,**” now entitled “**Carbon Dioxide and Methane Fluxes at the Air-Sea Interface of Red Sea Mangroves**” for publication reconsideration in *Biogeosciences*.

We would like to sincerely thank the reviewers for their suggestions, which have significantly improved the manuscript. We have attached a detailed response to the reviewers’ comments, noting all changes made to reflect their recommendations. We believe that these revisions have greatly improved the manuscript’s content and readability and hope you find this draft acceptable for publication in its present form.

Yours sincerely,

Sea and co-authors

46 We wish to sincerely thank reviewer #1 for his/her comments and suggestions that were very
47 helpful in improving and clarifying the MS.

48 Anonymous Referee #1:

49 Detailed comments

50
51 1. I focus here only on the methodology aspects since in my opinion the approach does not
52 measure CO₂ emission rates correctly, and the δ¹³C data are similarly not repre-
53 sentative. These concerns invalidate the discussion and conclusions on CO₂ fluxes and sources of CO₂.
54 The authors used 2 different experimental setups to perform their incubations. In both cases,
55 CO₂ fluxes are derived from an increase in the partial pressure of CO₂ in the water column
56 overlying the sediment in a sediment core; either by directly measuring pCO₂ in the water
57 (described in section 2.3.1) or by measuring pCO₂ in the headspace above the water column in a
58 sediment-water-headspace incu- bation (described in section 2.3.2). Both approaches assume that
59 all CO₂ produced in – and released from – the sediment accumulates as CO₂ in the overlying
60 water, and equilibrates with CO₂ in the headspace (for the 2nd approach), but ignores the fact
61 that dissolved CO₂ will rapidly equilibrate with dissolved HCO₃⁻ and CO₃²⁻ (see for example
62 Schulz et al. Marine Chemistry 100: 53-65 for a discussion on the kinetics of the inorganic
63 carbon equilibration). What should be determined is the change in the total DIC concentration,
64 rather than only looking at CO₂.

65 Reviewer one provides thought-provoking insights on carbonate chemistry in seawater, with
66 specific concerns focusing on the need to consider DIC fractionation in order to properly assess
67 the fluxes of DIC between sediment and water due to photosynthesis, respiration and numerous
68 Red-Ox processes.

69 We absolutely agree with the comment of reviewer 1, however, our intent is to measure the
70 fluxes at the air-sea interface, i.e. quantify the **net** GHG emissions to the atmosphere. It seems
71 that our language in several places made our intent more ambiguous than realized. Air-sea
72 equilibrators have been used in numerous studies to assess net CO₂ emissions by marine
73 ecosystems, such as in Borges et al., 2003 in inundated mangrove swamps.

74
75 In the new version of the MS, we make our scientific goals and interests more transparent
76 through numerous, related changes:

77
78 **Title**
79
80 The title has been changed to “**Carbon Dioxide and Methane Fluxes at the Air-Sea Interface**
81 **of Red Sea Mangroves**” to reflect this goal.

82
83 **Introduction**
84
85 We introduce the idea of measuring emissions in different ways in lines 74-78:
86 “Previous studies on GHG emission rates either focus on the soil-atmosphere interface,
87 highlighting substantial flux ranges with mangroves reported to act as negligible (Alongi, 2005)
88 to considerable sources (Livesley and Andrusiak, 2012; Chen et al., 2016), or examine net fluxes
89 at the air-sea interface, with few studies in arid systems.”

90

91 We clarify our goals in lines 87-90:

92
93 “Here we report air-sea emission rates of CO₂ and CH₄, along with their carbon isotopic
94 composition, from incubations of inundated mangrove sediments cores along the Saudi coast of
95 the Red Sea. We assess the relative role of these two gases in supporting total GHG emissions as
96 well as their fluctuations along the day-night cycle.”

97 98 **Discussion**

99
100 The discussion has now been divided into 2 subsections, the first of which addresses the
101 limitations of our methodology and subsequent comparison abilities (Lines 315-339):

102 103 *4.1 Greenhouse Gas Fluxes*

104
105 “While this study provides new insights on GHG fluxes from arid mangroves, the methods used
106 here solely measure the air-sea fluxes of dissolved gases. If CO₂ is produced from underlying
107 sediments, it enters the water column and becomes a part of the carbonate system, with
108 possibility of conversion to bicarbonate (HCO₃⁻) and carbonate (CO₃²⁻) ions; these dominating
109 species represent over 99% of the dissolved inorganic carbon (DIC) under current atmospheric
110 and oceanic conditions (Zeebe and Wolf-Gladrow, 2001). Therefore, the air-sea equilibration
111 methods used in this study do not measure DIC fluxes, but only the fluxes of the dissolved CO₂-
112 component of this larger system.

113
114 Frankignoulle and Borges (2001) show that CO₂ can be measured either directly (using
115 equilibrator techniques and spectroscopy or chromatography) or indirectly (by making
116 calculations based on pH, total alkalinity, and DIC). The methodology presented in this study
117 represents the former, utilizing an air-sea equilibrator connected to a CRDS to measure GHG
118 fluxes at the air-sea interface. Research conducted by Borges et al. (2003) utilizes the indirect
119 approach, using pH and total alkalinity measurements in Papua New Guinea to calculate DIC
120 and CO_{2(dis)} (for a computational discussion see Frankignoulle and Borges, 2001). Both methods
121 measure at the air-sea interface (Table Two) but are not directly comparable, as a full
122 determination of the carbonate system was not carried out in the present study. Similarly, studies
123 using equilibrator techniques that measure the dissolved CO₂ fraction of seawater to the
124 atmosphere are influenced by the seawater carbonate system and further steps of isotopic fraction
125 (discussed below), and are therefore not directly comparable to those studies which measure
126 GHG fluxes from exposed mangrove sediments to the atmosphere (Table Two).”

127
128 We delete the possibility of closing the carbon budget with our study (lines 31-33 and 303-309)
129 and add the possibility of future studies to do so (lines 299-305):

130 “Reported organic carbon burial rates of Red Sea mangroves of 3.42 mmol C m⁻² d⁻¹
131 (Almahasheer et al. 2017) are 10 times larger than the combined average CO₂ and CH₄ emission
132 rates reported here (0.37 mmol C m⁻² d⁻¹), suggesting that these mangrove sediments could act as
133 net atmospheric carbon sinks; however, significant annual alkalinity and DIC exports have been
134 identified from mangroves as well (Sippo et al., 2016), necessitating future studies which
135 measure these exports to neighboring habitats in order to close the carbon budget and determine
136 the role of Red Sea mangroves in potential climate change mitigation.”

137
138
139
140
141
142
143
144
145
146
147
148
149
150
151
152
153
154
155
156
157
158
159
160
161
162
163
164
165
166
167
168
169
170
171
172
173
174
175
176
177
178
179
180
181
182

Conclusion

Two concluding paragraphs have been added, tying together our thoughts and final remarks (lines 401-423). The second paragraph again addresses the limitations of our study (lines 415-423):

“Methods presented in this study include the use of an air-sea equilibrator connected to a CRDS to measure GHG fluxes at the air-sea interface, measuring the dissolved CO₂ component of the larger seawater carbonate system. This methodology is one of many used to measure GHG flux rates; establishing a unified sampling technique at both the soil-atmosphere and air-seawater interface will aid future researchers in determining total carbon budgets and accurately informing policymakers of their findings. In combination with consideration of isotope effects, a full determination of the carbonate system will be beneficial in future studies to further resolve GHG fluxes in arid mangroves, allowing us to better ascertain the role of these forests in global carbon budgets.”

Table Two

References in Table Two have been added, deleted, and reorganized to better reflect related studies:

Deleted

Kristensen et al., 2008a
Alongi, 2014
Chuang et al., 2015

Added

Borges et al., 2003
Bouillon et al., 2003
Bouillon et al., 2007a
Bouillon et al., 2007b
Bouillon et al., 2007c
Call et al., 2015
Ho et al., 2014
Jacotot et al. 2018
Rosentreter et al. 2018a
Rosentreter et al. 2018b

Changes have also been made to Table Two to distinguish between measurements made at the [1] soil-atmosphere interface, [2] air-sea interface with DIC calculation methods, and [3] air-sea interface with equilibration methods.

In addition to these alterations, smaller word choice changes were made throughout the document to clarify our intent:

Line 77: “examine net fluxes at the air-sea interface”

183 Line 128: “We measured CO₂ and CH₄ air-sea fluxes”

184 Line 238-239: “Inundated mangrove sediments”

185
186 2. Since there is isotope fractionation in the inorganic C system, with CO₂ being substantially
187 depleted in ¹³C relative to bicarbonate, the changes in d¹³C in CO₂ in the headspace are not
188 directly linked to the CO₂ produced in the sediment by respiration, but are transformed during
189 equilibration in the water column overlying the sediment, and there is an additional fractionation
190 step between aqueous (dissolved) and gaseous CO₂ (in the headspace). Hence, the Keeling plot
191 approach will not provide a reliable way of determining the source of CO₂ produced – both the
192 concentration and the d¹³C data determined in the authors’ approach are not relevant; it is the
193 total DIC concentration and d¹³C of the total DIC pool (or rather, DIC + CO₂ in headspace)
194 that should have been measured.

195 We concur with Reviewer #1’s thoughts and consequently discuss the limitation of our method,
196 acknowledging that our resulting d¹³C signals in the air phase comes after several steps of
197 isotopic segregation. This is done in the following places:

198

199 **Abstract**

200

201 We make conditional conclusions due to the limitations of our methods (Lines 24-29):

202

203 “Based on the isotopic composition of the CO₂ and CH₄ produced, we identified potential origins
204 of the organic matter that support GHG emissions. In all but one mangrove stand, GHG
205 emissions appear to be supported by organic matter from mixed sources, potentially reducing
206 CO₂ fluxes and instead enhancing CH₄ production, a finding that highlights the importance of
207 determining the origin of organic matter in GHG emissions”

208

209 **Discussion**

210

211 The discussion has now been divided into 2 subsections, the second of which addresses isotopic
212 segregation and its influence on our results (Lines 343-363):

213

214 *4.2 Isotopic Composition of Emitted Gases*

215

216 “There were no relationships between GHG fluxes and sediment properties, such as chlorophyll
217 *a*, nitrogen density, and organic carbon density, suggesting that other factors have greater
218 influence on GHG flux rates in this region. Since mangroves can receive large contributions of
219 organic carbon from other sources (Newell et al., 1995), such as algal mats, seagrass and
220 seaweed, examination of the isotopic composition of emitted carbon provides insights into the
221 origin of the organic carbon supporting GHG fluxes in mangrove sediments; however, it should
222 be noted that δ¹³C values reported in this study occur after several steps of isotopic fractionation
223 and may therefore influence results. Isotope effects can cause an unequal distribution of isotopes
224 between DIC components; for example as CO₂ is produced from mangrove sediments and
225 becomes part of the carbonate system (likely forming HCO₃⁻ after equilibration), molecules
226 containing the heavier carbon isotope—with a higher activation energy—will typically react
227 more slowly (Zeebe and Wolf-Gladrow, 2001), promoting a higher concentration of the heavy
228 isotope in unreacted CO₂ and a relative depletion of this heavier isotope in resulting HCO₃⁻.

229 Similarly, this preferential incorporation and movement of molecules containing lighter isotopes
230 can affect resulting carbon isotope ratios after air-sea equilibration (with depletion of lighter
231 isotopes in seawater as a result of fractionation). CO₂ measured in this study is subject to these
232 processes and may not reflect the isotopic ratios of carbon originally emitted; rather, the
233 signatures measured in this study should be seen as a proxy which reflects isotopic ratios of air-
234 sea discrimination and biological processing (decomposition, respiration, and photosynthesis)
235 resulting after carbon isotope fractionation. Interpretation of results is therefore subject to this
236 limitation.”

237

238 We also make conditional conclusions in this section due to the limitations of our methods :

239 Lines 380-385 : “Moreover, the mean isotopic signature of the CH₄ produced in mangrove
240 sediments ($\delta^{13}\text{C-CH}_4 = -80.6 \text{ ‰}$) tentatively confirms its biogenic origin”

241 Lines 387-389 : “The lowest $\delta^{13}\text{C-CH}_4$ was detected in S3, coinciding with the lowest $\delta^{13}\text{C-CO}_2$
242 value, suggesting that the organic matter being decomposed by methanogens likely came from
243 mangrove tissues as well”

244 Lines 392-397: “Organic matter with lighter isotopic composition could enhance CO₂ emissions,
245 whereas organic matter with heavier isotopic composition could enhance CH₄ emissions (Fig. 5),
246 possibly suggesting a different preferential use of organic matter by different microbial groups in
247 mangrove sediments. Future studies exploring this idea with further considerations of carbon
248 isotope fractionation would help solidify the role of the origin of organic carbon stored in
249 mangrove sediments on their GHG emissions.”

250 Lines 406-409 : “This study also highlights the importance of determining the source of organic
251 matter in GHG flux studies, as emissions appear to be supported by organic matter from mixed
252 sources in the majority of studied mangroves, potentially enhancing CH₄ production over CO₂
253 fluxes in this system.”

254

255

256

257

258

259

260

261

262

263

264 We would also like to thank reviewer #2 for his/her comments and suggestions that were very
265 helpful in improving and clarifying the MS.

266

267 Anonymous Referee #2:

268 1. Line 134 For cores S1 and S1, you need to factor in the equilibration time of the membrane
269 equilibrator as this would affect your rate calculations (Webb 2016 L&O). By not accounting for
270 equilibration time the flux estimates would underestimate emission rates.

271 We recognize that air-water equilibrators exhibit a delay in the measured response of gas
272 concentration and that, for some applications requiring exact CO₂ concentrations at a given time,
273 there is a need to deconvolve the CO₂ or CH₄ time series.

274 However, our study focused on rates, calculated as the slope during a phase in which we
275 observed a linear increase or decrease of gases for periods of 20 to 30 minutes. Convolution of
276 the time series due to lag would not affect those rates.

277

278 2. Line 46 Should be 12%

279 Line 46 (now line 49) was changed from 13% to 12%.

280

281 3. Line 198: Using the data in Table 1, I calculate a mean CO₂ flux of 1358 ± 1195 $\mu\text{mol m}^{-2}$
282 day^{-1}

283 It is possible that reviewer two calculated a mean CO₂ flux of $1358 \mu\text{mol m}^{-2} \text{day}^{-1}$ if he or she
284 accidentally plugged in +3452 for station 1 instead of -3452 for station 1. This would create a
285 mean CO₂ flux of 1358 instead of 372.

286

287 4. Line 201: You do not include the negative flux numbers in the reported range. I find the
288 variability of the source/sink behaviour of CO₂ at the different sites to be one of the most
289 interesting findings of the paper and there is limited speculation or use of the literature to suggest
290 why that may be. I would suggest a deeper interpretation is necessary. Factors including the
291 disturbance of sediments during coring may be particularly relevant as crab burrows would no
292 doubt be affected and coring through mangrove roots may disturb the entire sediment matrix.

293 We report the range of CO₂ fluxes observed to be -3452 to 7500 $\mu\text{mol CO}_2 \text{ m}^{-2} \text{ d}^{-1}$; it is
294 possible that reviewer two did not see the negative sign associated with -3452 as the negative
295 symbol appears on line 200 while the number 3452 appears on line 201. We moved the negative
296 sign down to the next line to make this more clear (now line 224). We wholeheartedly agree with
297 the reviewer's thoughts that the high degree of flux variability is an interesting finding and have
298 subsequently added our thoughts on this matter:

299

300 Lines 270-276: "Additionally it is possible that differences in flux rates may exist as a result of
301 sediment disturbance from the coring process. The effects of mangrove pneumatophores and
302 possible bioturbation from infaunal species such as burrowing crabs were not considered here yet
303 could pose another possible source of variation in results as the presence of these structures
304 influences oxygenation of sediment and pore water exchange, identified as driving factors in
305 varying CO₂ levels (Call et al., 2014; Rosentreter et al., 2018). These factors likely affect
306 relevant redox processes and would therefore be useful to quantify in future studies."

307

308 5. Line 202 It was 5 out of the 7 sites where daytime uptake and night time production was seen.
309 Line 202 was originally written to denote an overall observation, as the majority of sites
310 absorbed CO₂ during the day and emitted at night. We appreciate the reviewer's attention to
311 detail and have changed line 202 (now 226-227) to "Mangrove sediments absorbed CO₂ during
312 daytime and emitted CO₂ during night time at 5 out of 7 stations."

313

314 6. Line 203 the units should be $\mu\text{mol CO}_2 \text{ m}^{-2} \text{ hr}^{-1}$

315 We apologize for this error; units were corrected on line 203 (now 227).

316

317 7. Line 231 Averages and standard errors would be useful in Table 2
318 As noted above, we feel that one of the more interesting findings in our study (and similar
319 studies) is the wide variability in reported flux values. We choose to keep flux ranges in Table 2
320 and add averages (\pm SE) in the text as suggested (lines 260-265):
321
322 Values reported from this study fall within previously reported ranges for both CH₄ and CO₂, but
323 maximum CH₄ and CO₂ flux rates in the Red Sea are up to 100 fold below those reported
324 elsewhere. Compiled global values for GHG fluxes range from -16.9 to 629.2 mmol CO₂ m⁻² d⁻¹
325 and -2.1 to 25,974 μ mol CH₄ m⁻² d⁻¹, with mean (\pm SE) maximum emission rates averaging 202.3
326 \pm 48 mmol m⁻² d⁻¹ and 4783.6 \pm 2783 μ mol m⁻² d⁻¹ for CO₂ and CH₄ respectively (Table 2).
327
328 8. Line 231: Including a supplementary map of each field site would help delineate potential
329 differences between the sites.
330 While supplementary visuals would indeed aid in determining site differences, we unfortunately
331 did not record exact core locations, but instead noted distance away from the forest edge,
332 sampling near the center of the mangrove belt in each case. It was our hope that this would
333 minimize spatial differences; regardless we felt the need to include the possibility of spatial
334 variability in our discussion.
335
336 9. Line 263: Fix reference
337 As per the reviewer's suggestion, the referencing error was corrected (now line 376).

Carbon Dioxide and Methane Fluxes at the Air-Sea Interface of Red Sea Mangroves

Mallory A. Sea¹, Neus Garcias-Bonet¹, Vincent Saderne^{1*} and Carlos M. Duarte¹

[1] {King Abdullah University of Science and Technology (KAUST), Red Sea Research Center (RSRC), Thuwal, 23955-6900, Saudi Arabia}

*Correspondence to: V. Saderne (vincent.saderne@kaust.edu.sa)

Abstract

Mangrove forests are highly productive tropical and subtropical coastal systems that provide a variety of ecosystem services, including the sequestration of carbon. While mangroves are reported to be the most intense carbon sinks among all forests, they can also support large emissions of greenhouse gases (GHG), such as carbon dioxide (CO₂) and methane (CH₄), to the atmosphere. However, data derived from arid mangrove systems like the Red Sea are lacking. Here, we report net emission rates of CO₂ and CH₄ from mangroves along the eastern coast of the Red Sea, and assess the relative role of these two gases in supporting total GHG emissions to the atmosphere. Diel CO₂ and CH₄ emission rates ranged from -3452 to 7500 μmol CO₂ m⁻² d⁻¹ and from 0.9 to 13.3 μmol CH₄ m⁻² d⁻¹, respectively. The rates reported here fall within previously reported ranges for both CO₂ and CH₄, but maximum CO₂ and CH₄ flux rates in the Red Sea are 10 to 100-fold below those previously reported for mangroves elsewhere. Based on the isotopic composition of the CO₂ and CH₄ produced, we identified potential origins of the organic matter that support GHG emissions. In all but one mangrove stand, GHG emissions appear to be supported by organic matter from mixed sources, potentially reducing CO₂ fluxes and instead enhancing CH₄ production, a finding that highlights the importance of determining the origin of organic matter in GHG emissions. Methane was the main source of CO₂-equivalents despite the comparatively low emission rates in most of the sampled mangroves, and therefore deserves careful monitoring in this region. ~~Despite the mean net emission of CO₂ and CH₄ by~~

32 ~~Red Sea mangroves reported here, these forests become net organic carbon sinks when taking~~
33 ~~into account the existing carbon burial rates for Red Sea mangroves.~~ By further resolving GHG
34 fluxes in arid mangroves, we will better ascertain the role of these forests in global carbon
35 budgets.

36

37

38 1 Introduction

39

40 Mangrove forests, typically growing in the intertidal zones of tropical and subtropical coasts, are
41 highly productive components of coastal ecosystems and adapted to high salinity and anoxic
42 conditions associated with waterlogged sediments. Mangrove forests cover a global estimated
43 area of 137,760 km² (Giri et al., 2011) and are typically constrained by temperature, with
44 greatest biomass and species diversity in the equatorial zone (Alongi, 2012). Mangroves rank
45 amongst the most threatened ecosystems in the biosphere, with losses estimated at 50% of their
46 global extent over the past 50 years (Alongi, 2012). These losses affect nearly all mangrove
47 regions but the Red Sea, where mangrove coverage has increased by 12% over the past four
48 decades (Almahasheer et al., 2016).

49

50 Loss of mangrove forest represents a loss of valuable ecosystem services, including habitat and
51 nursery for marine species, coastal protection from erosion due to wave action, and the filtration
52 of harmful pollutants from terrestrial sources (Alongi, 2008), as well as loss of CO₂ sink
53 capacity. Additionally, mangroves can become a source of greenhouse gas (GHG) emissions
54 from disturbed soil carbon stocks (Donato et al., 2011; Alongi, 2014). Hence, mangrove
55 conservation and restoration have been proposed as important components of so-called Blue
56 Carbon strategies to mitigate climate change (Duarte, et al., 2013). Indeed, mangroves are
57 reported to be the most intense carbon sinks among all forests, supporting carbon sequestration
58 rates and organic carbon stocks as much as five times higher than those in terrestrial forests
59 (Donato et al., 2011). While mangrove forests cover less than 1% of total coastal ocean area,
60 they contribute to almost 15% of total carbon sequestration in coastal ecosystems (Alongi, 2012),
61 making mangrove forests highly effective in terms of carbon sequestration per unit area. The
62 management of mangroves to maximize CO₂ removal and subsequent storage is gaining
63 momentum as a cost-effective strategy to mitigate climate change.

64

65 However, mangrove forests act as both carbon sinks and sources and have been reported to
66 support large GHG emissions in the forms of CO₂ and CH₄ (Allen et al., 2007; Kristensen et al.,
67 2008a; Chen et al., 2016). Whereas concerns are focused on GHG emissions following mangrove
68 disturbance, estimated at 0.02 – 0.12 Pg C yr⁻¹ globally (Donato et al., 2011), undisturbed

69 mangrove sediments also support GHG emissions (Purvaja and Ramesh, 2000; Kristensen et al.,
70 2008b; Chauhan et al., 2015). Recent reports specifically highlight the importance of methane in
71 flux estimates, as emissions of CH₄, with a higher global warming potential, can offset mangrove
72 carbon burial by as much as 20% (Rosentreter et al., 2018b). Previous studies on GHG emission
73 rates either focus on the soil-atmosphere interface, highlighting substantial flux ranges~~mangrove~~
74 ~~sediments show highly variable fluxes,~~ with mangroves reported to act as negligible (Alongi,
75 2005) to considerable sources (Livesley and Andrusiak, 2012; Chen et al., 2016), or examine net
76 fluxes at the air-sea interface, with few studies in arid systems. Comparisons of carbon
77 sequestration rates between mangrove stands have revealed that climatic conditions play an
78 important role, with mangroves in the arid tropics, such as those in the Red Sea, supporting the
79 lowest carbon sequestration rates (Almahasheer et al. 2017). Likewise, GHG emissions from
80 mangrove forests may vary with climate, with most reported rates to-date derived from the wet
81 tropics (Alongi et al., 2005; Chauhan et al., 2015; Chen et al., 2016). Whereas Red Sea
82 mangroves are considered to play a minor role as CO₂ sinks, their role may be greater than
83 portrayed by low carbon burial rates if they also support very low GHG emissions, thereby
84 leading to a balance comparable to mangroves in the wet tropics.

85 Here we report air-sea emission rates of CO₂ and CH₄, along with their carbon isotopic
86 composition, from incubations of inundated mangrove sediments cores along the Saudi coast of
87 the Red Sea. We assess the relative role of these two gases in supporting total GHG emissions as
88 well as their fluctuations along the day-night cycle.

89

90 **2 Materials and Methods**

91

92 **2.1 Study area**

93

94 We sampled seven mangrove forests along the eastern coast of the Red Sea (Fig. 1). We
95 collected triplicate sediment cores by inserting translucent PVC tubes (30.5 cm in height and 9.5
96 cm in diameter) into mangrove sediments, collecting approx. 20 cm of sediment and a top
97 seawater layer. The overlying water was regularly replaced by fresh seawater from the
98 corresponding station in order to fill the remaining core volume and to measure CO₂ and CH₄
99 fluxes from underlying sediments during incubations. Mangrove sediments were sampled five to

100 ten meters from the forest edge, typically in the center of the mangrove belt. We sampled two
101 stations (S1 and S2) in January and February 2017 and the other five mangrove stations (S3-S7)
102 in March on board the R/V Thuwal as part of a scientific cruise. The cores collected from S1 and
103 S2 were immediately transported to the laboratory, placed in seawater baths and enclosed in
104 environmental growth chambers (Percival Scientific Inc., Perry, IA, USA) with 12:12 light
105 cycles at a constant temperature of 26°C. The sediment cores collected during the scientific
106 cruise were transported immediately on board and placed in open aquarium tanks with running
107 seawater in order to keep them close to *in situ* temperature. Salinity and temperature were
108 routinely recorded using a CTD. Additionally, sediment chlorophyll *a* and nutrient (organic
109 carbon and nitrogen) content were analyzed from cores collected during the scientific cruise.

110

111 **2.2 Sediment characteristics**

112

113 The chlorophyll *a* content of the sediment was measured by fluorometry. The surface layer of
114 each replicate core was collected and frozen until further analysis. Prior to chlorophyll *a*
115 extraction, the sediment samples were left at room temperature to thaw. The chlorophyll *a* was
116 extracted by adding 7 ml of 90% acetone to 2 ml of sediment sample. After a 24h incubation at
117 4° C in dark conditions, the samples were centrifuged and the chlorophyll *a* content in the
118 supernatant was measured on a Trilogy fluorometer. The nutrient (organic carbon and nitrogen)
119 content of the sediment was analyzed on an Organic Elemental Analyzer (Flash 2000) after
120 acidification of sediment samples.

121

122 **2.3 Measurement of greenhouse gas fluxes**

123

124 We measured CO₂ and CH₄ air-sea fluxes using two different techniques. The CO₂ and CH₄
125 fluxes from stations S1 and S2 were measured using the closed water circuit technique and the
126 CO₂ and CH₄ fluxes from the rest of the stations sampled during the scientific cruise (S3-S7)
127 were measured using the headspace technique.

128

129 **2.3.1 Measurement of CO₂ and CH₄ fluxes in sediment core incubations using** 130 **closed water circuit technique**

131
132 We incubated mangrove sediment cores from stations S1 and S2 using a closed water circuit
133 technique in order to measure changes in CO₂ and CH₄ concentrations. Before starting the
134 incubation, the seawater above the sediment from each core was replaced by fresh seawater
135 collected from the same location, avoiding disturbance of the sediment. Then, the seawater from
136 the core was recirculated by a peristaltic pump in an enclosed water circuit through a membrane
137 equilibrator (Liqui-cel mini module, 3M, Minnesota, USA). This setup enables the equilibration
138 of gases in dissolution with an enclosed air circuit. The air from the enclosed air circuit was then
139 passed through a desiccant column (calcium sulfate, WA Hammond Drierite Co., LTD, Ohio,
140 USA) and flowed into a cavity ring-down spectrometer (CRDS; Picarro Inc., Santa Clara, CA,
141 USA) to continuously measure the CO₂ and CH₄ concentration. We ran the incubations for at
142 least 30 minutes under light (200 μmol photons m⁻² s⁻¹) and dark conditions.

143

144 The concentration of CO₂ in the water circuit (μmol ml⁻¹) was calculated by Eq. (1):

$$145 \quad [\text{CO}_2] = H_{cp} \times [\text{HP_CO}_2] \times (1 - p_{\text{H}_2\text{O}}), \quad (1)$$

146 where H_{cp} is the Henry constant (mol ml⁻¹ atm⁻¹) calculated using R marelac package (Soetaert
147 et al., 2016); $[\text{HP_CO}_2]$ is the given concentration of CO₂ (ppm), and $p_{\text{H}_2\text{O}}$ is the water vapor
148 pressure (atm).

149 The CO₂ fluxes were calculated from the change in CO₂ concentration over time during our
150 incubations, correcting by the seawater volume present in each core. Then, the fluxes were
151 transformed to an aerial basis (μmol m⁻² h⁻¹) by taking into account the core surface area. Finally,
152 the daily fluxes (μmol m⁻² d⁻¹) were calculated by multiplying the CO₂ flux obtained under light
153 conditions by the number of light hours plus the CO₂ flux obtained under dark conditions by the
154 number of dark hours.

155 The CH₄ fluxes were calculated in the same manner as for the CO₂ fluxes, with the exception
156 that the Henry constant was calculated using Eq. (2):

$$157 \quad \beta = H_{cp} \times (RT), \quad (2)$$

158 where H_{cp} is the Henry constant ($\text{mol ml}^{-1} \text{atm}^{-1}$), R is the ideal gas constant (82.057338 atm ml
159 $\text{mol}^{-1} \text{K}^{-1}$), T is standard temperature (273.15 K), and β is the Bunsen solubility coefficient of
160 CH_4 , extracted from Wiesenburg and Guinasso (1979).

161 **2.3.2 Measurement of CO_2 and CH_4 fluxes in sediment core incubations using the** 162 **headspace technique**

163 Mangrove sediment cores from stations S3 to S7 were incubated using a headspace technique in
164 order to measure changes in CO_2 and CH_4 concentrations. Before starting the incubation, the
165 seawater above the sediment from each core was replaced by fresh seawater from the running
166 seawater system, leaving a headspace of 200 ml. Each core was sealed with a stopper equipped
167 with a gas-tight valve serving as a headspace sampling port. The sealed core was left for 1 hour
168 before the first headspace sampling to allow equilibration between seawater and air phases. Each
169 core was sampled with a syringe, withdrawing 15 ml of air from the equilibrated headspace.
170 Headspace samples were periodically drawn from each sediment incubation over a 24-hour
171 incubation period. The CO_2 and CH_4 concentrations in the headspace samples along with their
172 isotopic composition ($\delta^{13}\text{C}-\text{CO}_2$ and $\delta^{13}\text{C}-\text{CH}_4$) were measured with a CRDS (Picarro Inc., Santa
173 Clara, CA, USA) connected to a small sample isotopic module extension (SSIM A0314, Picarro
174 Inc., Santa Clara, CA, USA). We ran standards (730 ppm CO_2 , 1.9 ppm CH_4) before and after
175 every three samples.

176 The concentration of dissolved CO_2 in the seawater after equilibrium was calculated from the
177 concentration in the equilibrated headspace (ppm) as described previously by Wilson et al.
178 (2012) for other gases:

$$179 \quad [\text{CO}_2]_w = 10^{-6} \beta m_a p_{dry}, \quad (3)$$

180 where β is the Bunsen solubility coefficient of CO_2 ($\text{mol ml}^{-1} \text{atm}^{-1}$), m_a is the given
181 concentration of CO_2 in the equilibrated headspace (ppm), and p_{dry} is atmospheric pressure (atm)
182 of dry air. The Bunsen solubility coefficient of CO_2 was calculated using Eq. (4):

$$183 \quad \beta = H_{cp} \times (RT) \quad (4)$$

184 where H_{cp} is the Henry constant ($\text{mol ml}^{-1} \text{ atm}^{-1}$) calculated using R marelac package (Soetaert
185 et al., 2016), R is the ideal gas constant ($82.057338 \text{ atm ml mol}^{-1} \text{ K}^{-1}$) and T is standard
186 temperature (273.15 K). The atmospheric pressure of dry air (p_{dry}) was calculated using Eq. (5):

$$187 \quad p_{dry} = p_{wet} (1 - \%H_2O) \quad (5)$$

188 where p_{wet} is the atmospheric pressure of wet air corrected by the effect of multiple syringe
189 draws from the same core, applying Boyle's law.

190 The initial concentration of dissolved CO_2 in seawater before equilibrium was then calculated as:

$$191 \quad [\text{CO}_2]_{aq} = ([\text{CO}_2]_w V_w + 10^{-6} m_a V_a) / V_w \quad (6)$$

192 where $[\text{CO}_2]_w$ is the concentration of dissolved CO_2 in the seawater after equilibrium, V_w is the
193 volume of seawater (ml) and V_a is the headspace volume (ml) in the core. Finally, treating the
194 gas as ideal, the units were converted to nM using Eq. (7):

$$195 \quad [\text{CO}_2]_{aq} = 10^9 * p_{dry} [\text{CO}_2]_{aq} / (RT) \quad (7)$$

196 where R is the ideal gas constant ($0.08206 \text{ atm l mol}^{-1} \text{ K}^{-1}$) and T is temperature (K).

197 The CO_2 fluxes were calculated from the change in CO_2 concentration over time during our
198 incubations, correcting by the seawater volume present in each core. Then, the fluxes were
199 transformed to an aerial basis ($\mu\text{mol m}^{-2} \text{ d}^{-1}$) by taking into account the core surface area. Finally,
200 the day and night fluxes ($\mu\text{mol m}^{-2} \text{ h}^{-1}$) were calculated from the change in CO_2 concentration
201 between consecutive samplings during day and night time, respectively.

202 The CH_4 fluxes were calculated in the same manner as for the CO_2 fluxes, with the exception
203 that the Bunsen solubility coefficient of CH_4 was calculated according to Wiesenburg and
204 Guinasso (1979).

205

206 **2.4 Isotopic composition of CO_2 ($\delta^{13}\text{C}$ - CO_2) and CH_4 ($\delta^{13}\text{C}$ - CH_4)**

207

208 The isotopic signature of the CO₂ and CH₄ produced [during](#) incubations was estimated by
209 conducting keeling plots (Pataki et al. 2003; Thom et al. 2003; Garcias-Bonet and Duarte 2017).
210 Briefly, the δ¹³C of the CO₂ and CH₄ produced was extracted from the intercept of the linear
211 regression between the inverse of the gas partial pressure and the isotopic signature.

212
213 [The data set is available from Sea et al. \(2018\).](#)
214

215 **3 Results**

216
217 The mean (± SE) diel CO₂ and CH₄ emission rates for the seven sites were 372 ± 1309 μmol CO₂
218 m⁻² d⁻¹ and 5.6 ± 1.6 μmol CH₄ m⁻² d⁻¹, respectively. We observed high variability among the
219 seven mangrove forest sites studied, with net CO₂ and CH₄ diel emission rates ranging from
220 -3452 to 7500 μmol CO₂ m⁻² d⁻¹ and from 0.9 to 13.3 μmol CH₄ m⁻² d⁻¹, respectively (Table 1).
221

222 Mangrove sediments absorbed CO₂ during daytime and emitted CO₂ during night time [at 5 out of](#)
223 [7 stations](#), with means (± SE) of -54.6 ± 37 μmol CO₂ m⁻² h⁻¹ and 86 ± 120 μmol CO₂ m⁻² h⁻¹
224 respectively (Table 1, Fig. 2). However, in three out of seven sites, heterotrophic activities
225 outbalanced photosynthesis on a 24h basis. At two sites, S3 and S6, we found an increase of the
226 CO₂ emissions between day and night, contradictory to the classical daytime primary
227 production–night-time respiration pattern, possibly indicative of a light mediated increase of
228 heterotrophic processes.

229
230 Methane emissions did not show circadian patterns with linear increases in CH₄ concentration in
231 our incubations (Fig. 2) and with similar light and dark rates (0.26 ± 0.08 and 0.21 ± 0.07 μmol
232 CH₄ m⁻² h⁻¹ (mean ± SE), respectively (Table 1). In terms of total GHG contribution, the mean
233 CO₂-equivalents (CO₂e) emission [to the atmosphere](#) was 564 ± 1284 μmol CO₂e m⁻² d⁻¹ (mean ±
234 SE) [using the 100 years' time horizon global warming potential \(Myhre et al., 2013\)](#). [Inundated](#)
235 mangrove sediments were net emitters of CO₂e in three out of seven sites (Table 1), and in five
236 out of seven mangrove stands sampled, CH₄ was the main source of CO₂e to the atmosphere.
237

238 While no overall trend was revealed through the relationship between day and night fluxes for
239 CO₂ and CH₄ (Fig. 3), consistencies are evident at specific mangrove stations. For example,
240 night CO₂ emissions are clearly visible at S2, while S3 appears to emit CO₂ during daylight
241 hours. No relationship was apparent between GHG fluxes and the densities of organic carbon or
242 nitrogen in the sediment. There was no discernible trend between gas fluxes and chlorophyll *a*
243 content in surface sediments.

244
245 The isotopic signatures of the produced CO₂ ($\delta^{13}\text{C-CO}_2$) ranged from -11.21 to -25.72 ‰ as
246 derived from keeling plots (Fig. 4, Table 1). The $\delta^{13}\text{C-CO}_2$ was similar for almost all stations,
247 with the exception of S3 that had a $\delta^{13}\text{C-CO}_2$ of -25.72 ‰. The isotopic composition of the
248 produced CH₄ ($\delta^{13}\text{C-CH}_4$) ranged from -71.28 to -87.08 ‰, with a mean $\delta^{13}\text{C}$ signature of -80.61
249 ‰ (Fig. 4, Table 1).

250

251 **4 Discussion**

252

253 **4.1 Greenhouse gas fluxes**

254

255 The CO₂ and CH₄ emissions reported in this study show that Red Sea mangroves can act as a
256 source of GHG to the atmosphere. Values reported from this study fall within previously
257 reported ranges for both CH₄ and CO₂, but maximum CH₄ and CO₂ flux rates in the Red Sea are
258 up to 100 fold below those reported elsewhere. Compiled global values for GHG fluxes range
259 from -16.9 to 629.2 mmol CO₂ m⁻² d⁻¹ and -2.1 to 25,974 μmol CH₄ m⁻² d⁻¹, with mean (±SE)
260 maximum emission rates averaging 202.3 ± 48 mmol m⁻² d⁻¹ and 4783.6 ± 2783 μmol m⁻² d⁻¹ for
261 CO₂ and CH₄ respectively (Table 2).

262

263 The variability in GHG emission rates reported in this study could be attributed to spatial
264 differences, as cores were taken from different parts of each forest. Indeed, previous studies
265 report significant discrepancies in emission rates in fringe versus forest positions (Allen et al.,
266 2007). Additionally it is possible that differences in flux rates may exist as a result of sediment
267 disturbance from the coring process. The effects of mangrove pneumatophores and possible
268 bioturbation from infaunal species such as burrowing crabs were not considered here yet could

269 pose another possible source of variation in results as the presence of these structures influences
270 oxygenation of sediment and pore water exchange, identified as driving factors in varying CO₂
271 levels (Call et al., 2014; Rosentreter et al., 2018). These factors likely affect relevant redox
272 processes and would therefore be useful to quantify in future studies.

273
274 Uniformity of day and night emission rates for CH₄ was observed in Red Sea mangrove stands,
275 with mean (\pm SE) CH₄ emission rates of $0.28 \pm 0.08 \mu\text{mol CH}_4 \text{ m}^{-2} \text{ h}^{-1}$ during the day and $0.24 \pm$
276 $0.08 \mu\text{mol CH}_4 \text{ m}^{-2} \text{ h}^{-1}$ during night; this is consistent with previous work reporting that emission
277 rates for CH₄ do not vary significantly during light and dark hours in mangrove forests (Allen et
278 al., 2007). It has been suggested instead that variables such as sediment temperature are more
279 significant in their contributions to emission rates (Allen et al., 2007; Allen et al., 2011).
280 Incubated sediment cores kept at constant temperature do not reflect the range of temperatures
281 experienced by mangrove sediments over the diurnal cycle; future studies examining GHG
282 emissions under more realistic temperature fluctuations are needed. Seasonal studies of longer
283 duration have reported increased emission rates during warmer seasons (Chen et al., 2016;
284 Livesley and Andrusiak, 2012). Methane concentrations typically remain low due to anaerobic
285 methane oxidation processes that take place near sediment surfaces (Kristensen et al., 2008a),
286 consistent with the low CH₄ emission rates from Red Sea mangrove sediments observed here.
287 Additionally, environments of high salinity like the Red Sea have been associated with decreased
288 CH₄ emissions, as sulfate-reducing bacteria are thought to outcompete methanogens
289 (Poffenbarger et al., 2011).

290
291 Methane emission rates at the air-sea interface of Red Sea mangrove sediments, although quite
292 low, become more substantial when considered in terms of global warming potential. In this
293 study, CH₄ was, despite the comparatively low emission rates, the main source of CO₂e in the
294 majority of sampled mangroves, and therefore deserves careful monitoring in this region.
295 Reported organic carbon burial rates of Red Sea mangroves of $3.42 \text{ mmol C m}^{-2} \text{ d}^{-1}$
296 (Almahasheer et al. 2017) are 10 times larger than the combined average CO₂ and CH₄ emission
297 rates reported here ($0.37 \text{ mmol C m}^{-2} \text{ d}^{-1}$), suggesting that these mangrove sediments could act as
298 net atmospheric carbon sinks; however, significant alkalinity and DIC exports have been
299 identified from mangroves as well (Sippo et al., 2016), necessitating future studies which

300 measure these exports to neighboring habitats in order to close the carbon budget and determine
301 the role of Red Sea mangroves in potential climate change mitigation. Currently, protection
302 measures and further reforestation efforts are being deployed along the Red Sea that will further
303 expand the area of mangroves (Almhasheer et al. 2016). The rationale for conserving mangroves
304 in the climate change context is not adequately represented by their net carbon sink capacity
305 when undisturbed, but rather by the emissions resulting from their disturbance. Indeed, previous
306 studies analyzing anthropogenic impacts on methane emission rates from mangrove sediments
307 have shown that disturbance significantly increases methane emissions (Purvaja and Ramesh,
308 2001; Chen et al., 2011). This provides an additional rationale to conserve, and continue to
309 expand, Red Sea mangroves.

310
311 While this study provides new insights on GHG fluxes from arid mangroves, the methods used
312 here solely measure the air-sea fluxes of dissolved gases. If CO₂ is produced from underlying
313 sediments, it enters the water column and becomes a part of the carbonate system, with
314 possibility of conversion to bicarbonate (HCO₃⁻) and carbonate (CO₃²⁻) ions; these dominating
315 species represent over 99% of the dissolved inorganic carbon (DIC) under current atmospheric
316 and oceanic conditions (Zeebe and Wolf-Gladrow, 2001). Therefore, the air-sea equilibration
317 methods used in this study do not measure DIC fluxes, but only the fluxes of the dissolved CO₂.
318 component of this larger system.

319
320 Frankignoulle and Borges (2001) show that CO₂ can be measured either directly (using
321 equilibrator techniques and spectroscopy or chromatography) or indirectly (by making
322 calculations based on pH, total alkalinity, and DIC). The methodology presented in this study
323 represents the former, utilizing an air-sea equilibrator connected to a CRDS to measure GHG
324 fluxes at the air-sea interface. Research conducted by Borges et al. (2003) utilizes the indirect
325 approach, using pH and total alkalinity measurements in Papua New Guinea to calculate DIC
326 and CO₂(dis) (for a computational discussion see Frankignoulle and Borges, 2001). Both methods
327 measure at the air-sea interface (Table Two) but are not directly comparable, as a full
328 determination of the carbonate system was not carried out in the present study. ~~of our study et al.~~
329 ~~(2003)~~ Similarly, studies using equilibrator techniques that measure the dissolved CO₂ fraction
330 of seawater to the atmosphere are influenced by the seawater carbonate system and further steps

331 of isotopic fraction (discussed below), and are therefore not directly comparable to those studies
332 which measure GHG fluxes from exposed mangrove sediments to the atmosphere (Table Two).

333 fully

334 **4.2 Isotopic composition of emitted gases**

335
336 There were no relationships between GHG fluxes and sediment properties, such as chlorophyll *a*,
337 nitrogen density, and organic carbon density, suggesting that other factors have greater influence
338 on GHG flux rates in this region. Since mangroves can receive large contributions of organic
339 carbon from other sources (Newell et al., 1995), such as algal mats, seagrass and seaweed,
340 examination of the isotopic composition of emitted carbon provides insights into the origin of the
341 organic carbon supporting GHG fluxes in mangrove sediments; however, it should be noted that
342 $\delta^{13}\text{C}$ values reported in this study occur after several steps of isotopic fractionation and may
343 therefore influence results. Isotope effects can cause an unequal distribution of isotopes between
344 DIC components; for example as CO_2 is produced from mangrove sediments and becomes part
345 of the carbonate system (likely forming HCO_3^- after equilibration), molecules containing the
346 heavier carbon isotope—with a higher activation energy—will typically react more slowly
347 (Zeebe and Wolf-Gladrow, 2001), promoting a higher concentration of the heavy isotope in
348 unreacted CO_2 and a relative depletion of this heavier isotope in resulting HCO_3^- . Similarly, this
349 preferential incorporation and movement of molecules containing lighter isotopes can affect
350 resulting carbon isotope ratios after air-sea equilibration (with depletion of lighter isotopes in
351 seawater as a result of fractionation). CO_2 measured in this study is subject to these processes
352 and may not reflect the isotopic ratios of carbon originally emitted; rather, the signatures
353 measured in this study should be seen as a proxy which reflects isotopic ratios of air-sea
354 discrimination and biological processing (decomposition, respiration, and photosynthesis),
355 resulting after carbon isotope fractionation. Interpretation of results is therefore subject to this
356 limitation.

357
358 The isotopic signature of the CO_2 ($\delta^{13}\text{C}\text{-CO}_2$) produced by mangrove sediments in four out of the
359 five mangrove stands with available isotopic data was heavier (from -11.2 ± 0.6 to -15.9 ± 1.1
360 ‰; Table 1) than the isotopic signature of mangrove tissues, suggesting decomposition of
361 organic matter from mixed sources (Kennedy et al. 2010). Specifically, the isotopic signature of

362 the mangroves found in the central Red Sea has been recently reported as $\delta^{13}\text{C}_{\text{leaves}} = -26.98 \pm$
363 0.15 ‰ , $\delta^{13}\text{C}_{\text{stems}} = -25.75 \pm 0.16 \text{ ‰}$ and $\delta^{13}\text{C}_{\text{roots}} = -24.90 \pm 0.17 \text{ ‰}$ for mangrove leaves, stems
364 and roots while the mean isotopic signature of other primary producers in the central the Red Sea
365 has been reported as $\delta^{13}\text{C}_{\text{seaweed}} = -12.8 \pm 0.5 \text{ ‰}$ and $\delta^{13}\text{C}_{\text{seagrass}} = -8.2 \pm 0.2 \text{ ‰}$ for seaweed and
366 seagrass tissues, respectively (Almahasheer et al. 2017). However, in one mangrove stand (S3)
367 the $\delta^{13}\text{C}\text{-CO}_2$ was much lighter ($-25.72 \pm 0.21 \text{ ‰}$), potentially indicating mangrove tissues. Thus,
368 according to the isotopic signature, the CO_2 produced in mangrove sediments would be
369 supported by mangrove biomass in only one mangrove stand out of the five sampled sites with
370 available isotopic data. Moreover, the mean isotopic signature of the CH_4 produced in mangrove
371 sediments ($\delta^{13}\text{C}\text{-CH}_4 = -80.6 \text{ ‰}$) tentatively confirms its biogenic origin, which normally ranges
372 from -40 to -80 ‰ , depending on the isotopic signature of the organic compounds being
373 biologically decomposed (Reeburgh, 2014). The lowest $\delta^{13}\text{C}\text{-CH}_4$ was detected in S3, coinciding
374 with the lowest $\delta^{13}\text{C}\text{-CO}_2$ value, suggesting that the organic matter being decomposed by
375 methanogens likely came from mangrove tissues as well.

376
377 Interestingly, the mangrove with the lightest $\delta^{13}\text{C}\text{-CO}_2$ and $\delta^{13}\text{C}\text{-CH}_4$ (S3), showed the lowest
378 daily CO_2 flux ($-1524 \pm 686 \mu\text{mol CO}_2 \text{ m}^{-2} \text{ d}^{-1}$) but the highest CH_4 emission rate (13.3 ± 9.5
379 $\mu\text{mol CH}_4 \text{ m}^{-2} \text{ d}^{-1}$), compared to the fluxes detected in the rest of mangrove stands with available
380 isotopic data. Part of the variability in the CO_2 ($R^2 = 0.42$) and CH_4 ($R^2 = 0.40$) emission rate
381 seems to be explained by the origin of the organic matter being decomposed, estimated here as
382 the $\delta^{13}\text{C}\text{-CO}_2$ and $\delta^{13}\text{C}\text{-CH}_4$. Organic matter with lighter isotopic composition could enhance
383 CO_2 emissions, whereas organic matter with heavier isotopic composition could enhance CH_4
384 emissions (Fig. 5), possibly suggesting a different preferential use of organic matter by different
385 microbial groups in mangrove sediments. Future studies exploring this idea with further
386 considerations of carbon isotope fractionation would help solidify the role of the origin of
387 organic carbon stored in mangrove sediments on their GHG emissions.

388 389 **5 Conclusion**

390
391 This study is first in reporting CO_2 and CH_4 fluxes from Red Sea mangrove sediments,
392 contributing to the scant data on arid mangrove systems (Atwood et al. 2017, Almahasheer et al.

393 2017), essential to establish a solid baseline on GHG emissions for future studies. Results show
394 that maximum CO₂ and CH₄ flux rates from Red Sea mangrove sediments are well below those
395 reported elsewhere, and that, even when considered in terms of CO₂ equivalents, carbon burial
396 rates largely outweigh GHG emission rates at the air-sea interface in this region. This study also
397 highlights the importance of determining the source of organic matter in GHG flux studies, as
398 emissions appear to be supported by organic matter from mixed sources in the majority of
399 studied mangroves, potentially enhancing CH₄ production over CO₂ fluxes in this system.
400 Seasonal variation should be considered in future studies on GHG emissions by Red Sea
401 mangroves to better determine annual emission rates from this system, which reaches some of
402 the warmest temperatures experienced by mangrove forests worldwide. Similarly, a wider spatial
403 coverage within the mangrove forest should be considered to confidently determine net GHG
404 fluxes that can be upscaled to the entire stock of Red Sea mangroves.

405 Methods presented in this study include the use of an air-sea equilibrator connected to a CRDS to
406 measure GHG fluxes at the air-sea interface, measuring the dissolved CO₂ component of the
407 larger seawater carbonate system. This methodology is one of many used to measure GHG flux
408 rates; establishing a unified sampling technique at both the soil-atmosphere and air-seawater
409 interface will aid future researchers in determining total carbon budgets and accurately informing
410 policymakers of their findings. In combination with consideration of isotope effects, a full
411 determination of the carbonate system will be beneficial in future studies to further resolve GHG
412 fluxes in arid mangroves, allowing us to better ascertain the role of these forests in global carbon
413 budgets.

414

415 *Data availability.* All data will be accessible in the repository Pangea pending manuscript
416 acceptance.

417

418 *Competing interests.* The authors declare that they have no conflict of interest.

419

420 **Author contribution**

421 MAS, NG-B, VS and CMD designed the study. MAS and NG-B performed the measurements
422 and calculations. MAS, NG-B, VS and CMD interpreted the results. All authors contributed
423 substantially to the final manuscript.

424

425 **Acknowledgements**

426

427 This research was funded by King Abdullah University of Science and Technology (KAUST)
428 through baseline funding to C.M.D. We thank D. Krause-Jensen, ~~Nabeel-N.~~ Massoudi, and
429 ~~Kimberlee-K. Baldree-Baldry~~ for help during sampling, and the captain and crew of KAUST R/V
430 Thuwal for support. M.A.S. was supported by King Abdullah University of Science and
431 Technology through the VRSP program. We thank P. Carrillo de Albornoz for lab instrument
432 support, and ~~Mongi-M.~~ Ennasri for help with sediment analysis.

433

434 **References**

435

436 Allen, D. E., Dalal, R. C., Rennenberg, H., Meyer, R., L., Reeves, S., and Schmidt, S.: Spatial
437 and temporal variation of nitrous oxide and methane flux between subtropical mangrove
438 sediments and the atmosphere, *Soil. Biol. Biochem.*, 39, 622-631, 2007.

439

440 Allen, D. E., Dalal, R.C., Rennenberg, H., and Schmidt, S.: Seasonal variation in nitrous oxide
441 and methane emissions from subtropical estuary and coastal mangrove sediments, Australia,
442 *Plant. Biol.*, 13, 126-133, 2011.

443

444 Almahasheer, H., Aljowair, A., Duarte, C. M., and Irigoien, X.: Decadal stability of Red Sea
445 mangroves, *Estuar. Coast. Shelf. S.*, 169, 164-172, 2016.

446

447 Almahasheer, H., Serrano, O., Duarte, C. M., Arias-Ortiz, A., Masque, P., and Irigoien, X.: Low
448 carbon sink capacity of Red Sea mangroves, *Scientific Reports*, 7, 9700, doi:10.1038/s41598-
449 017-10424-9, 2017.

450

451 Alongi, D. M.: Mangrove forests: Resilience, protection from tsunamis, and responses to global
452 climate change, *Estuar. Coast. Shelf. S.*, 76, 1-13, 2008.

453

454 Alongi, D. M.: *The energetics of mangrove forests*, Springer Press, London, England, 2009.

455

456 Alongi, D. M.: Carbon sequestration in mangrove forests, *Carbon. Manag.*, 3, 313-322, doi:
457 10.4155/cmt.12.20, 2012.

458

459 Alongi, D. M.: Carbon cycling and storage in mangrove forests, *Annu. Rev. Mar. Sci.*, 6, 195-
460 219, doi: 10.1146/annurev-marine-010213-135020, 2014.

461

462 Alongi, D. M., Pfitzner, J., Trott, L. A., Tirendi, F., Dixon, P., and Klumpp, D. W.: Rapid
463 sediment accumulation and microbial mineralization in forests of the mangrove *Kandelia candel*
464 in the Jiulongjiang Estuary, China, *Estuar. Coast. Shelf. S.*, 63, 605-618, 2005.

465 Atwood, T. B., Connolly, R. M., Almahasheer, H., Carnell, P., Duarte, C. M., Ewers, C.,
466 Irigoien, X., Kelleway, J., Lavery, P. S., Macreadie, P. I., Serrano, O., Sanders, C., Santos, I.,
467 Steven, A., and Lovelock, C. E.: Global patterns in mangrove soil carbon stocks and losses, *Nat.*
468 *Clim. Change*, 7, 523-529, doi:10.1038/nclimate3326, 2017.

469
470 Borges, A. V., Djenidi, S., Lacroix, G., Theate, J., Delille, B., and Frankignoulle, M.:
471 Atmospheric CO₂ flux from mangrove surrounding waters, *Geophys. Res. Lett.*, 30, 1558,
472 doi:10.1029/2003GL017143, 2003.

473
474 Bouillon, S., Frankignoulle, M., Dehairs, F., Velimirov, B., Eiler, A., Gwenael, A., Etcheber, H.,
475 and Borges, A. V.: Inorganic and organic carbon biogeochemistry in the Gautami Godavari
476 estuary (Andhra Pradesh, India) during pre-monsoon: The local impact of extensive mangrove
477 forests, *Global. Biogeochem. Cy.*, 17, 1114, doi:10.1029/2002GB002026, 2003.

478
479 Bouillon, S., Dehairs, F., Schiettecatte, L., and Alberto Vieira Borges, A. V.: Biogeochemistry of
480 the Tana estuary and delta (northern Kenya), *Limnol. Oceanogr.*, 52, 46-59, 2007a.

481
482 Bouillon, S., Dehairs, F., Velimirov, B., Gwenael, A., and Borges, A. V.: Dynamics of organic
483 and inorganic carbon across contiguous mangrove and seagrass systems (Gazi Bay, Kenya), *J.*
484 *Geophys. Res.*, 112, G02018, doi:10.1029/2006JG000325, 2007b.

485
486 Bouillon, S., Middelburg, J. J., Dehairs, F., Borges, A. V., Abril, G., Flindt, M. R., Ulomi, S.,
487 and Kristensen, E.: Importance of intertidal sediment processes and porewater exchange on the
488 water column biogeochemistry in a pristine mangrove creek (Ras Dege, Tanzania),
489 *Biogeosciences*, 4, 317-348, 2007c.

490
491 Call, M., Maher, D. T., Santos, I. R., Ruiz-Halpern, S., Mangion, P., Sanders, C. J., Erler, D. V.,
492 Oakes, J. M., Rosentreter, J., Murray, R., and Eyre, B. D.: Spatial and temporal variability of
493 carbon dioxide and methane fluxes over semi-diurnal and spring-neap-spring timescales in a
494 mangrove creek, *Geochimica et Cosmochimica Acta*, 150, 211-225, 2015.

495 Chauhan, R., Datta, A., Ramanathan, A. L., and Adhya, T. K.: Factors influencing spatio-
496 temporal variation of methane and nitrous oxide emission from a tropical mangrove of eastern
497 coast of India, *Atmos. Environ.*, 107, 95-106, 2015.

498 Chen, G., Tam, N. F. Y., Wong, Y. S., and Ye, Y.: Effect of wastewater discharge on greenhouse
499 gas fluxes from mangrove soils, *Atmos. Environ.*, 45, 1110-1115, 2011.

500

501 Chen, G., Chen, B., Yu, D., Tam, N. F. Y., Ye, Y., and Chen, S.: Soil greenhouse gas emissions
502 reduce the contribution of mangrove plants to the atmospheric cooling effect, *Environ. Res. Lett.*,
503 11,1-10, doi:10.1088/1748-9326/11/12/124019, 2016.

504

505 Duarte, C. M., Losada, I. J., Hendriks, I. E., Mazarrasa, I., and Marbà, N.: The role of coastal
506 plant communities for climate change mitigation and adaptation, *Nat. Clim. Change*, 3, 961-968,
507 doi: 10.1038/NCLIMATE1970, 2013.

508

509 Donato, D. C., Kauffman, J. B., Murdiyarso, D., Kurnianto, S., Stidham, M., and Kanninen, M.:
510 Mangroves among the most carbon-rich forests in the tropics, *Nat. Geosci.*, 4, 293-297, doi:
511 10.1038/NGEO1123, 2011.

512

513 [Frankignoulle, M., and Borges, A. V.: Direct and indirect pCO₂ measurements in a wide range of](#)
514 [pCO₂ and salinity values \(the Scheldt Estuary\), *Aquat. Geochem.*, 7, 267-273, 2001.](#)

515

516 Garcias-Bonet, N. and Duarte, C. M.: Methane production by seagrass ecosystems in the Red
517 Sea, *Frontiers in Marine Science*, 4, 340, doi: 10.3389/fmars.2017.00340, 2017.

518

519 Giri, C., Ochieng, E., Tieszen, L. L., Zhu, Z., Singh, A., Loveland, T., Masek, J., and Duke, N.:
520 Status and distribution of mangrove forests of the world using earth observation satellite data,
521 *Global. Ecol. Biogeogr.*, 20, 154-159, 2011.

522

523 [Ho, D. T., Ferrón, S., Engel, V. C., Larsen, L. G., and Barr, J.G.: Air-water gas exchange and](#)
524 [CO₂ flux in a mangrove-dominated estuary, *Geophys. Res. Lett.*, 41, 108-113,](#)
525 [doi:10.1002/2013GL058785, 2014.](#)

526

527 [Jacotot, A., Marchand, C., and Allenbach, M.: Tidal variability of CO₂ and CH₄ emissions from](#)
528 [the water column within a Rhizophora mangrove forest \(New Caledonia\), Sci. Total. Environ.,](#)
529 [631, 334-340, 2018.](#)

530

531 Kanninen, M.: Mangroves among the most carbon-rich forests in the tropics, *Nat. Geosci.*, 4,
532 293-297, doi:10.1038/ngeo1123, 2011.

533

534 Kennedy, H., Beggins, J., Duarte, C. M., Fourqurean, J. W., Holmer, M., Marbà, N., and
535 Middelburg, J. J.: Seagrass sediments as a global carbon sink: isotopic constraints, *Global*
536 *Biogeochem. Cy.*, 24, GB4026, doi: 10.1029/2010GB003848, 2010.

537

538 Kristensen, E., Bouillon, S., Dittmar, T., and Marchand, C.: Organic carbon dynamics in
539 mangrove ecosystems: A review, *Aquat. Bot.*, 89, 201-219, doi:10.1016/j.aquabot.2007.12.005,
540 2008a.

541

542 Kristensen, E., Flindt, M. R., Ulomi, S., Borges, A. V., Abril, G., and Bouillon, S.: Emissions of
543 CO₂ and CH₄ to the atmosphere by sediments and open waters in two Tanzanian mangrove
544 forests, *Mar. Ecol. Prog. Ser.*, 370, 53-67, doi: 10.3354/meps07642, 2008b.

545

546 Livesley, S. J., and Andrusiak, S. M.: Temperate mangrove and salt marsh sediments are a small
547 methane and nitrous oxide source but important carbon store, *Estuar. Coast. Shelf. Sci.*, 97, 19-
548 27, 2012.

549

550 Myhre, G., Shindell, D., Bréon, F. M., Collins, W., Fuglestedt, J., Huang, J., Koch, D.,
551 Lamarque, J. F., Lee, D., Mendoza, B., and Nakajima, T.: Anthropogenic and natural radiative
552 forcing, *Climate Change*, 423, 2013.

553

554 Newell, R. I. E., Marshall, N., Sasekumar, A., and Chong, V. C.: Relative importance of benthic
555 microalgae, phytoplankton, and mangroves as sources of nutrition for penaeid prawns and other
556 coastal invertebrates from Malaysia, *Mar. Biol.*, 123, 595-606, 1995.

557
558 Pataki, D., Ehleringer, J. R., Flanagan, L. B., Yakir, D., Bowling, D. R., Still, C. J., Buchmann,
559 N., Kaplan, J. O., and Berry, J. A.: The application and interpretation of Keeling plots in
560 terrestrial carbon cycle research, *Global. Biogeochem. Cy.*, 17, 1022, doi:
561 10.1029/2001GB001850, 2013.
562
563 Poffenbarger, H. J., Needelman, B. A., and Megonigal, J. P.: Salinity influence on methane
564 emissions from tidal marshes, *Wetlands*, 31, 831-842, doi: 10.1007/s13157-011-0197-0, 2011.
565 Purvaja, R. and Ramesh, R.: Human impacts on methane emission from mangrove ecosystems in
566 India, *Reg. Environ. Change.*, 1, 86-97, doi: 10.1007/PL00011537, 2000.
567
568 Purvaja, R. and Ramesh, R.: Natural and anthropogenic methane emission from wetlands of
569 south India, *Environ. Manage.*, 27, 547-557, doi: 10.1007/s002670010169, 2001.
570 Reeburgh, W. S.: *Global Methane Biogeochemistry Treatise on Geochemistry (Second Edition)*,
571 Holland, H. D., and Turekian, K. K., Oxford, Elsevier, 71-94, 2014.
572
573 [Rosentreter, J. A., Maher, D. T., Erler, D. V., Murray, R., and Eyre, B. D.: Seasonal and](#)
574 [temporal CO₂ dynamics in three tropical mangrove creeks- A revision of global mangrove CO₂](#)
575 [emissions, *Geochimica et Cosmochimica Acta*, 222, 729-745, 2018a.](#)
576
577 [Rosentreter, J. A., Maher, D. T., Erler, D. V., Murray, R. H., and Eyre, B. D. Methane emissions](#)
578 [partially offset “blue carbon” burial in mangroves, *Sci. Adv.*, 4, eaao4985, 2018b.](#)
579
580 Sea, M. A., Garcias-Bonet, N., Saderne, V., and Duarte, C. M.: Data set on methane emissions
581 from Red Sea mangrove sediments. Pangea DOI: [data set will be published in the Pangea open
582 data repository at the acceptance of paper], 2018.
583
584 [Sippo, J. Z., Maher, D. T., Tait, D. R., Holloway, C., and Santos, I. R.: Are mangroves drivers or](#)
585 [buffers of coastal acidification? Insights from alkalinity and dissolved inorganic carbon export](#)
586 [estimates across a latitudinal transect, *Global. Biogeochem. Cy.*, 30: 753-766, 2016.](#)

587 Soetaert, K., Petzoldt, T., and Meysman, F.: Marelac: A tool for aquatic sciences (R package),
588 available at: <https://cran.r-project.org/web/packages/marelac/marelac.pdf>, 2016.

589

590 Thom, M., Bosinger, R., Schmidt, M., and Levin, I.: The regional budget of atmospheric
591 methane of a highly populated area, *Chemosphere*, 26, 143-160, doi: 10.1016/0045-
592 6535(93)90418-5, 1993.

593

594 Wiesenburg, D. A. and Guinasso, N. L.: Equilibrium solubilities of methane, carbon monoxide,
595 and hydrogen in water and sea water, *J. Chem. Eng. Data.*, 24, 356-360, 1979.

596

597 Wilson, S. T., Böttjer, D., Church, M. J., and Karla, D. M.: Comparative assessment of nitrogen
598 fixation methodologies, conducted in the oligotrophic north Pacific Ocean, *Appl. Environ.*
599 *Microb.*, 78, 6516-6523, 2012.

600

601 [Zeebe, R. E. and Wolf-Gladrow, D. A.: CO2 in seawater: equilibrium, kinetics, isotopes,](#)
602 [Elsevier, Amsterdam, 2001.](#)

603

604

605

606

607

608

609

610

611

612

613

614

615

616

617

618 FIGURE HEADINGS

619

620 **Fig. 1.** Mangrove stands sampled along the Saudi coast of the Red Sea. Numbers indicate
621 positions of sampling sites from this study. S1 and S2: King Abdullah University of Science and
622 Technology; S3: Duba; S4 and S5: Al Wahj; S6 and S7: Farasan Banks.

623

624 **Fig. 2.** Change in CO₂ (left panels) and CH₄ (right panels) concentrations over time in triplicated
625 mangrove sediment cores from mangrove stations S3-S7. Shaded areas represent night time and
626 each replicate is coded by different symbols.

627

628 **Fig. 3.** Relationship between day and night fluxes for CO₂ (top panel) and CH₄ (bottom panel) at
629 all mangrove stations.

630

631 **Fig. 4.** Keeling plots for mangrove stations S3-S7, showing the linear regression of the inverse of
632 CO₂ concentration (left panels) and CH₄ concentration (right panels) versus $\delta^{13}\text{C}-\text{CO}_2$ and $\delta^{13}\text{C}-$
633 CH₄. Y-intercepts were used to estimate the isotopic signatures of produced gases.

634

635 **Fig. 5.** Relation between the carbon isotopic signature of the produced CO₂ ($\delta^{13}\text{C}-\text{CO}_2$) and CO₂
636 fluxes (top panel) and carbon isotopic signature of the produced CH₄ ($\delta^{13}\text{C}-\text{CH}_4$) and the CH₄
637 fluxes (bottom panel) in Red Sea mangroves. Error bars indicate standard error of the mean.

638

639

640

641

642

643

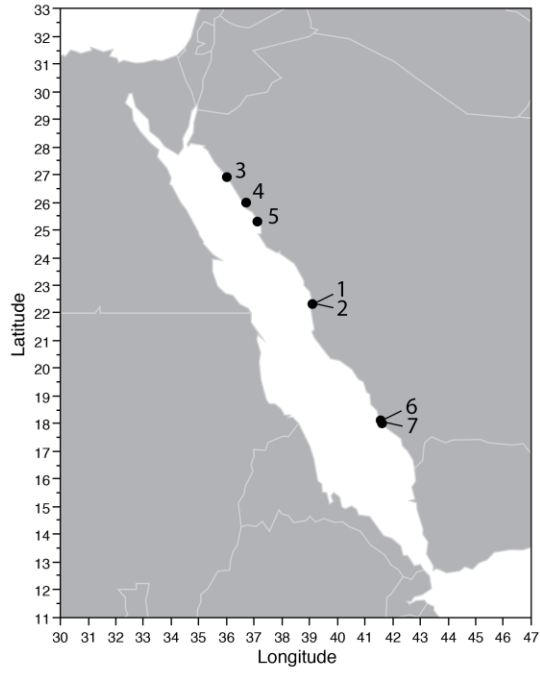
644

645

646

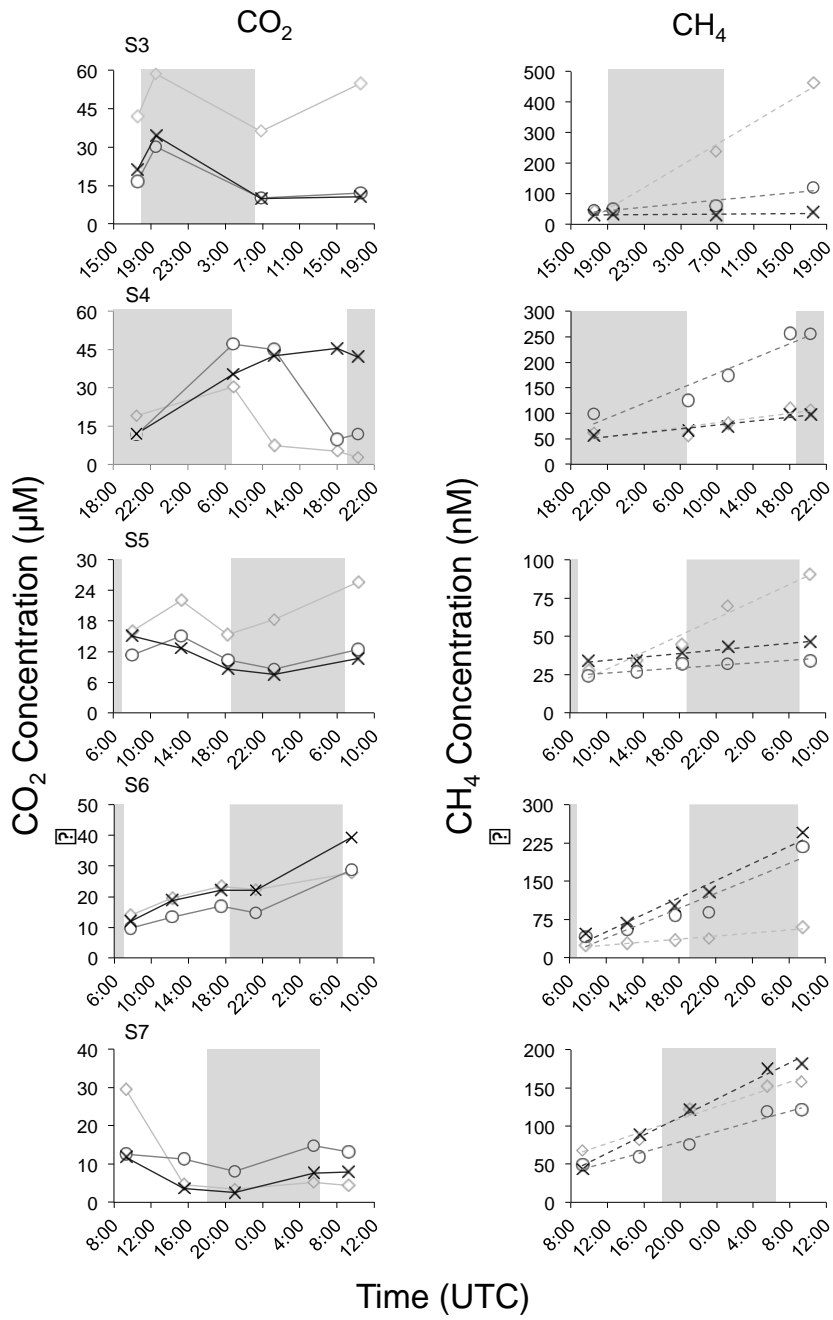
647

648 **Figure 1**



649
650
651
652
653
654
655
656
657

658 **Figure 2**



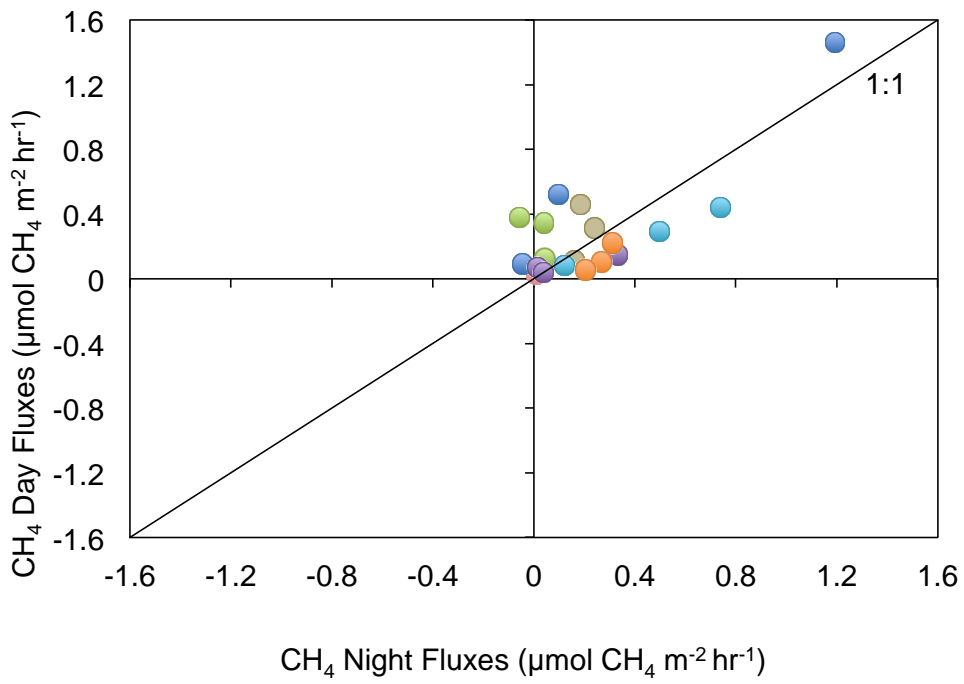
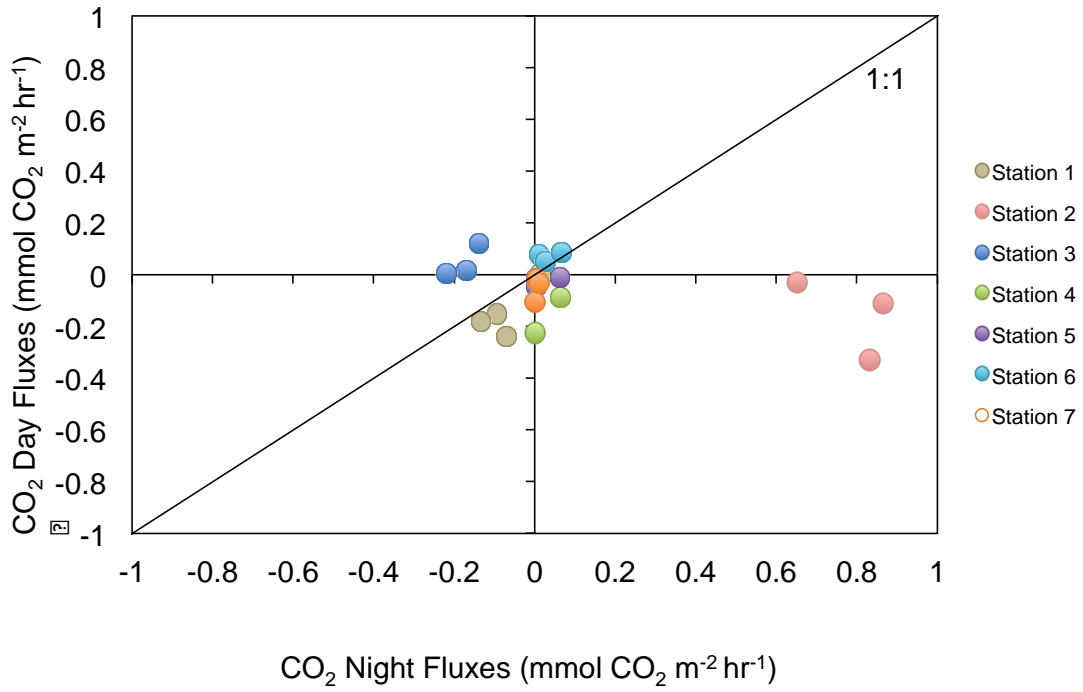
659

660

661

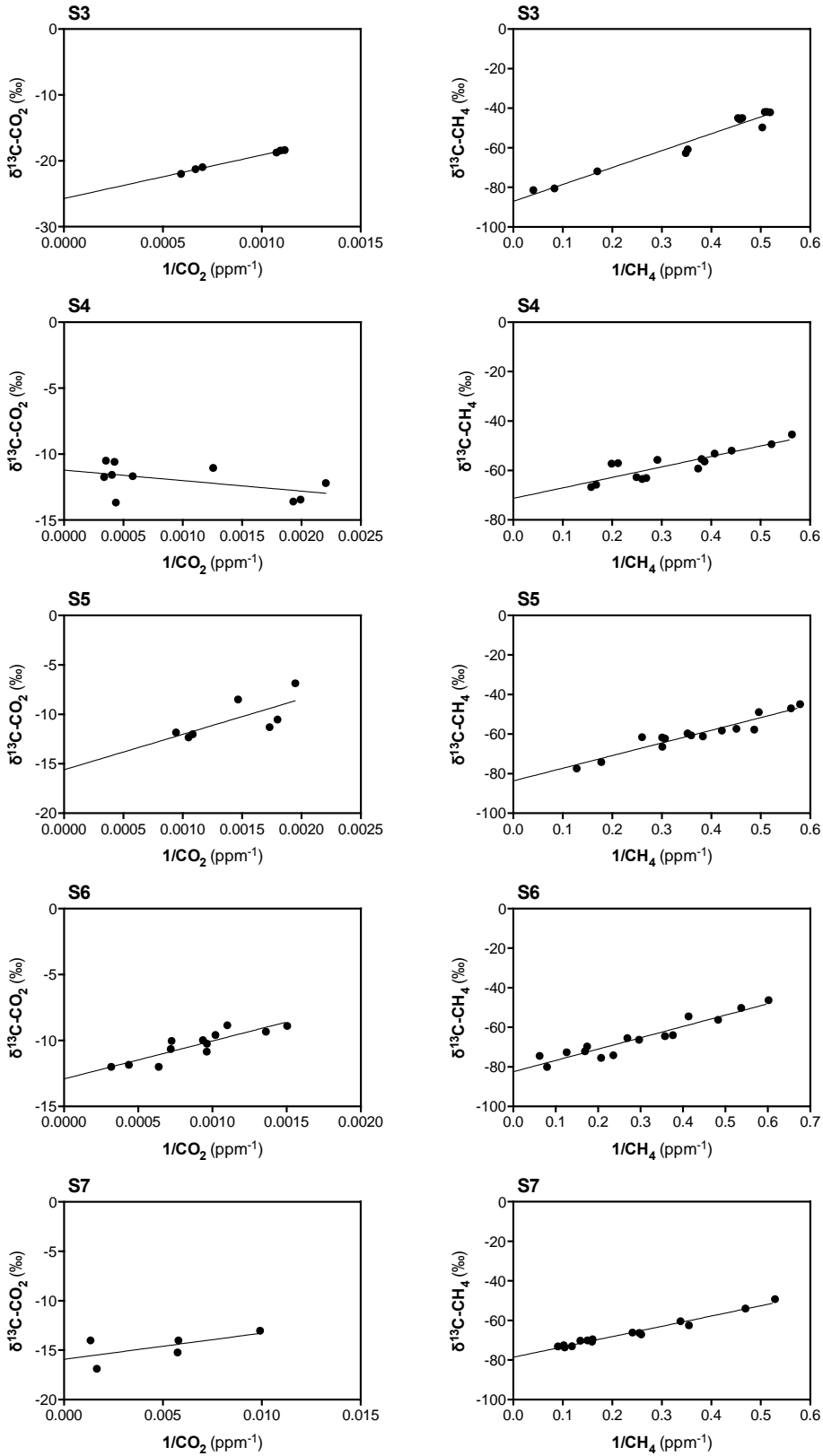
662 **Figure 3**

663



664

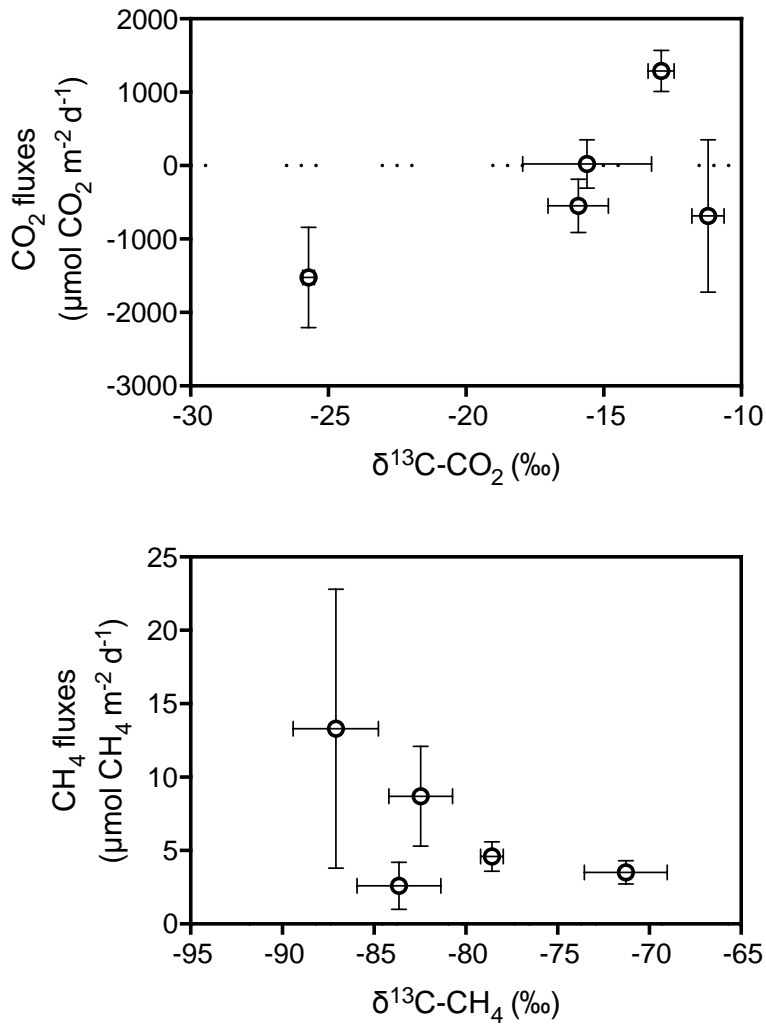
665



668 **Figure 5**

669

670



671

Table 1. Summary of greenhouse gas fluxes and sediment characteristics from studied mangrove forests. CH₄ fluxes in brackets represent CO₂ equivalents in terms of global warming potential for a time horizon of 100 years (GWP₁₀₀), taking into account climate-carbon feedback as suggested by the AR5 of IPCC (Myhre et al., 2013). Data represent the mean ± SEM and nd means no data available.

Station	CO ₂ Day Flux (μmol CO ₂ m ⁻² hr ⁻¹)	CH ₄ Day Flux (μmol CH ₄ m ⁻² hr ⁻¹)	CO ₂ Night Flux (μmol CO ₂ m ⁻² hr ⁻¹)	CH ₄ Night Flux (μmol CH ₄ m ⁻² hr ⁻¹)	Daily CO ₂ Flux (μmol CO ₂ m ⁻² d ⁻¹)	Daily CH ₄ Flux (μmol CH ₄ m ⁻² d ⁻¹)	δ ¹³ C-CO ₂ (‰)	δ ¹³ C-CH ₄ (‰)	Nitrogen Density (mgN cm ⁻²)
1	-188 ± 25	0.30 ± 0.17 [10.2]	-99 ± 18	0.19 ± 0.04 [6.46]	-3452 ± 271	5.9 ± 1.3 [201]	nd	nd	nd
2	-157 ± 89	0.05 ± 0.02 [1.7]	782 ± 66	0.03 ± 0.01 [1.02]	7500 ± 894	0.9 ± 0.25 [31]	nd	nd	nd
3	49 ± 37	0.69 ± 0.4 [23.46]	-176 ± 23	0.42 ± 0.39 [14.28]	-1524 ± 686	13.3 ± 9.5 [452]	-25.7 ± 0.2	-87.1 ± 2.3	1.03 ± 0.0
4	-86 ± 79	0.28 ± 0.1 [9.52]	29 ± 19	0.01 ± 0.03 [0.34]	-684 ± 1038	3.5 ± 0.8 [119]	-11.1 ± 0.6	-71.3 ± 2.3	0.80 ± 0.0
5	-22 ± 11	0.09 ± 0.03 [3.06]	24 ± 20	0.13 ± 0.10 [4.42]	23 ± 331	2.6 ± 1.6 [88]	-15.6 ± 2.3	-83.6 ± 2.3	1.12 ± 0.0
6	73 ± 10	0.27 ± 0.10 [9.18]	35 ± 17	0.45 ± 0.18 [15.30]	1289 ± 280	8.7 ± 3.4 [296]	-12.9 ± 0.5	-82.5 ± 1.7	1.51 ± 0.1
7	-51 ± 28	0.13 ± 0.05 [4.42]	5 ± 3	0.26 ± 0.03 [8.84]	-547 ± 363	4.6 ± 1.0 [156]	-15.9 ± 1.1	-78.6 ± 0.6	3.30 ± 0.5

Table 2. Comparison of GHG fluxes from global mangrove forests and Red Sea mangroves. Literature values converted from reported form for comparison purposes. Measurements made at the: 1. soil-atmosphere interface, 2. air-sea interface with DIC calculation methods, and 3. air-sea interface with equilibration methods.

			CO ₂ (mmol m ⁻² d ⁻¹)		CH ₄ (μmol m ⁻² d ⁻¹)	
Author	Year	Place	Minimum	Maximum	Minimum	Maximum
Allen et	2007	Australia	=	=	4.5	25974

<u>al.¹Kristensen</u>						
<u>Allen et al.¹</u>	<u>2011</u>	<u>Australia</u>	<u>=</u>	<u>=</u>	<u>70.3</u>	<u>2348</u>
<u>Alongi et al.¹</u>	<u>2005</u>	<u>China</u>	<u>17</u>	<u>121</u>	<u>5</u>	<u>66</u>
<u>Chen et al.¹</u>	<u>2016</u>	<u>China</u>	<u>-16.9</u>	<u>279.2</u>	<u>-2.1</u>	<u>8015.1</u>
<u>Kristensen et al.^{1,2}</u>	<u>2008b</u>	<u>Tanzania</u>	<u>28</u>	<u>115</u>	<u>0</u>	<u>87.6</u>
<u>Livesley & Andrusiak¹</u>	<u>2012</u>	<u>Australia</u>	<u>50</u>	<u>150</u>	<u>50</u>	<u>749</u>
<u>Borges et al.²</u>	<u>2003</u>	<u>Papua New Guinea</u>	<u>=</u>	<u>43.6</u>	<u>=</u>	<u>=</u>
<u>Bouillon et al.²</u>	<u>2003</u>	<u>India</u>	<u>=</u>	<u>70.2</u>	<u>=</u>	<u>=</u>
<u>Bouillon et al.²</u>	<u>2007a</u>	<u>Kenya</u>	<u>3</u>	<u>252</u>	<u>=</u>	<u>=</u>
<u>Bouillon et al.²</u>	<u>2007b</u>	<u>Kenya</u>	<u>=</u>	<u>52</u>	<u>=</u>	<u>=</u>
<u>Bouillon et al.²</u>	<u>2007c</u>	<u>Tanzania</u>	<u>1</u>	<u>80</u>	<u>=</u>	<u>=</u>
<u>Call et al.³</u>	<u>2015</u>	<u>Australia</u>	<u>9.4</u>	<u>629.2</u>	<u>13.1</u>	<u>632.9</u>
<u>Ho et al.³</u>	<u>2014</u>	<u>United States</u>	<u>20</u>	<u>118</u>	<u>=</u>	<u>=</u>
<u>Jacotot et al.³</u>	<u>2018</u>	<u>New Caledonia</u>	<u>3.12</u>	<u>441.8</u>	<u>4.32</u>	<u>4129.7</u>
<u>Rosentreter et al.³</u>	<u>2018a</u>	<u>Australia</u>	<u>58.7</u>	<u>277.6</u>	<u>=</u>	<u>=</u>
<u>Rosentreter et al.³</u>	<u>2018b</u>	<u>Australia</u>	<u>=</u>	<u>=</u>	<u>96.5</u>	<u>1049.8</u>
<u>This Study³</u>	<u>2017</u>	<u>Red Sea</u>	<u>-3.5</u>	<u>7.5</u>	<u>0.9</u>	<u>13.3</u>